Chapter 14
Forced Vibration Harmonic Response Analysis of Semi-mobile Crusher Station

Shanmugam Perumal, Raghunathan Swaminathan and Mike Christensen

Abstract The objective of the analysis was to design SMC structure to withstand dynamic loading condition due to crusher operation. A study about forced vibration analysis for Semi-mobile crusher (SMC) using finite element analysis (FEA) was carried out to determine the natural frequencies, mode shapes and forced harmonic frequency response characteristics. Natural frequency analysis and followed by harmonic frequency response analysis were performed using finite element calculations to find out critical frequencies and its corresponding peak displacements and dynamic stresses. The results of the study show the weakest direction and critical frequencies of the structure. Also, the dynamic displacement and stresses were found to be acceptable thereby the structural dynamic integrity of the SMC structure was established.

Keywords Semi-mobile crusher · Modal analysis · Frequency response analysis · Effective mass participation · Critical frequencies

14.1 Introduction

FLSmidth relocatable crushing stations were designed to significantly reduce truck haulage and help realize the many benefits of in-pit crushing and conveying. The result is reduced operating costs and environmental impact. The SMC series of modular crushing stations allows for quick relocations and comes available with a gyratory crusher that can reduce any type of feed material to a conveyable size. To

S. Perumal (✉) · R. Swaminathan
FLSmidth India Private Limited, Chennai, India
e-mail: shanmugam.perumal@flsmidth.com

R. Swaminathan
e-mail: raghunathan.swaminathan@flsmidth.com

M. Christensen
FLSmidth USA Inc, Salt Lake City, USA
e-mail: Mike.Christensen@flsmidth.com

C. Li et al. (eds.), *Advances in Engineering Design and Simulation*,
Lecture Notes on Multidisciplinary Industrial Engineering,
https://doi.org/10.1007/978-981-13-8468-4_14

determine the dynamic response of the SMC structure under a steady-state sinusoidal (harmonic) loading due to gyratory crusher at a given frequency, forced vibration harmonic response analysis was carried out.

14.2 Semi-mobile Crusher Station

The semi-mobile crusher (SMC) station was constructed from structural steel and consists of four major sections: the crusher module, two (2) truck bridges and the discharge conveyor. The crusher module was designed to be moved as a single unit except for the truck bridges. The truck bridges were designed to be moved in sections. The discharge conveyor was designed to be moved as a single unit. Figure 14.1 shows the semi-mobile crusher station's description.

The semi-mobile crusher frame was primarily made out of ASTM A36. The property values for this material were listed in Table 14.1.

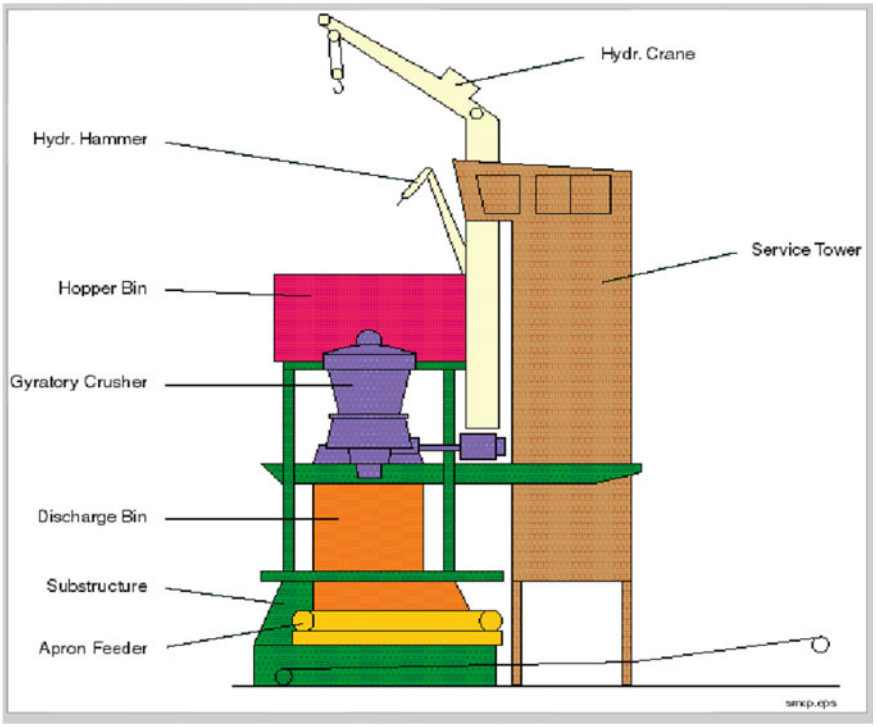

Fig. 14.1 Semi-mobile crusher station description

Table 14.1 Material properties for the Semi-mobile crusher frame

Property	Value
Density (Kg/m^3)	7850
Young's modulus (GPa)	200
Poisson's ratio	0.26
Yield strength (MPa)	250
Endurance strength (MPa)	150

14.3 Assumptions

Material considered was homogeneous. Material considered was linear elastic and isotropic. Nonlinear due to geometry was not considered in the analysis. Overall structural constant damping was assumed as 5%. Welds were modelled as a node to node connectivity at the interface locations. Gyratory crusher, rock breaker, crane, motor and other auxiliary equipment were modelled as point masses and will be connected to the respective mounting points. Mode superposition method was followed for the frequency response analysis.

14.4 Modal Analysis

The mode shapes and frequency directly impact the dynamic response of the system to dynamic inputs such as produced by rotating equipment like the gyratory crusher and motor, wind loads, earthquakes, etc. The modal analysis results of the semi-mobile frame were summarized in the table. The first 50 natural frequencies were reported based on effective mass participation.

14.4.1 Finite Element (FE) Model

The FE model consists of four noded shell elements. The weld locations were modelled as a node to node connectivity. The total number of nodes 2,283,917 and total number elements was 2,309,721. The mass of the FE model was 943 tonnes.

14.4.2 Loads and Boundary Condition

The crusher, crane, rock breaker, crusher motor, and Lub & Hydraulic Skid and Miscellaneous Equipment were modelled as a lumped point mass at their approximate

Table 14.2 Mass details of different equipment

Location	Assembly/equipment	Mass (T)
A	Crusher	310
B	Crane	41
C	Rock breaker	27
D	Crusher motor	12
E	Lub and Hydraulic skid and Miscellaneous equipment	11
–	Structural steel frame	943
	Total	1344

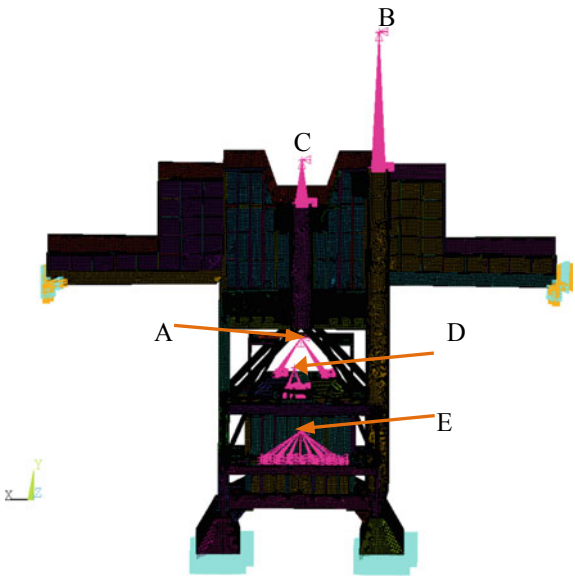

Fig. 14.2 Semi-mobile crusher—loads and boundary condition

CG locations and connected to their respective mounting locations through rigid connections. Table 14.2 shows the mass details of all equipment/assembly considered.

The bottom faces of the pontoons were constrained in translations in all three directions and rotations were free. Two extreme edges of the truck bridge were constrained with fixed support (All translations and rotations constrained) as shown in Fig. 14.2.

14.5 Significance of Effective Mass Participation

The significance of the vibration mode was represented by effective mass participation. It was a measure of how much energy gets into a mode leading to larger

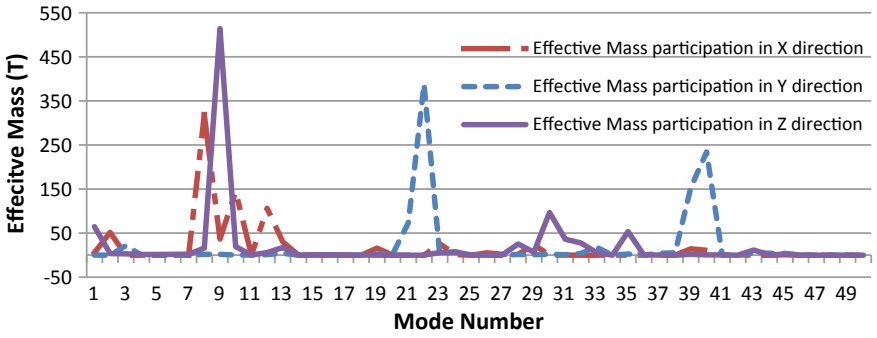

Fig. 14.3 Effective mass participation

Table 14.3 Effective mass participation percentage

Direction	Total mass (T)	Modal effective mass (T)	Percentage
X	1344	801	60
Y	1344	950	71
Z	1344	941	70

amplitudes. Modes with relatively high effective masses can be readily excited by excitation. On the other hand, modes with low effective masses cannot be readily excited (Fig. 14.3 and Table 14.3).

Effective mass participation in *X* direction indicates that more effective mass was observed in the first 30 modes. Thereafter, the incremental mass was observed in the remaining modes. Effective mass participation in *Y* direction indicates that more effective mass was observed between 20th modes and 40th modes. Effective mass participation in *Z* direction indicates that more effective mass was observed between 1st mode and 15th mode and between 25th mode and 35th mode.

14.6 Natural Frequencies

There were 50 natural frequencies captured based on effective mass participation. The reason behind capturing 50 modes was to capture 80% of the total effective mass. But, even after capturing 100 modes, we could not reach 80% mass participation as after 50th mode only incremental mass captured and it was about less than 5%. Hence it was decided to limit the number of modes into 50 modes to reduce the solution time and without compromising much on the accuracy. Figure 14.4 shows the natural frequencies captured for first 50 modes. The first fundamental natural frequency was 1.36 Hz and there were three natural frequencies lower than 2.3 Hz.

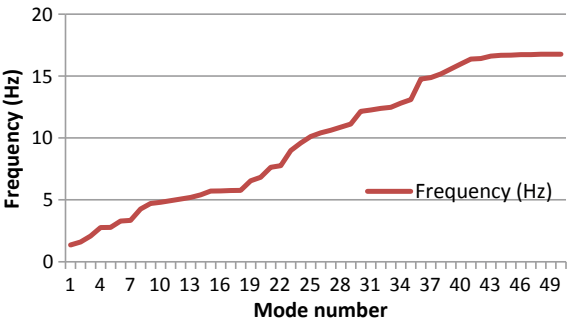

Fig. 14.4 Natural frequencies

14.7 Frequency Response (Harmonic) Analysis

The harmonic analysis was a technique used to determine the steady-state response of a linear structure to loads that vary sinusoidally (harmonically) with time. The idea was to calculate the structure's response at several frequencies and obtain a graph of some response quantity (usually displacements) versus frequency. "Peak" responses were then identified on the graph and stress reviewed at those peak frequencies.

Crusher unbalanced force of 197.9 KN was applied in the *X* direction to simulate force vibration response on the SMC station structure

14.7.1 Locations Identified for Displacement Measurement Over Frequency Range

To identify critical forcing frequencies—frequencies at which the highest displacements (or stresses) occur at points of interest in the model will be selected—and to then post-process the entire model at these critical forcing frequencies (Fig. 14.5).

14.7.1.1 Location 1

This location was chosen based on the mode shape 1 where this particular location might deform more as compared to other locations. The node number corresponds to this location was 666,830 in the crane mounting support.

14.7.1.2 Location 2

This location was chosen based on the mode shape 3 where this particular location might deform more as compared to other locations. The node number corresponds to this location was 233,597 in the feed hopper (crane side).

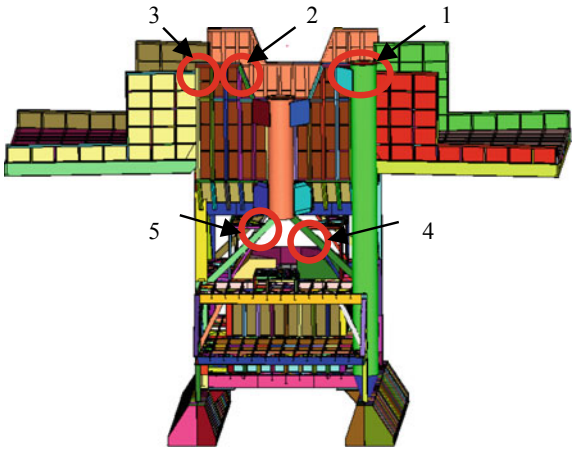

Fig. 14.5 Locations considered for displacement measurement

14.7.1.3 Location 3

This location was chosen based on the mode shape 8. The node number corresponds to this location was 233494 in the feed hopper (crane side).

14.7.1.4 Location 4

This location was chosen based on the mode shape 9, 10, 12 and 13. The node number corresponds to this location was 796,567 in the feed hopper (crane side).

14.7.1.5 Location 5

This location was chosen based on the mode shape 9, 10, 12 and 13. The node number corresponds to this location was 795,948 in the feed hopper (crane side).

14.7.2 Max Displacement Plots for X Direction Unbalanced Forces

See Tables 14.4, 14.5 and 14.6.

Table 14.4 Max displacement for *X* direction unbalanced forces

Location	Displacement in *X* direction (mm)	Displacement in *Y* direction (mm)	Displacement in *Z* direction (mm)
1	2.60	0.11	1.90
2	2.37	0.64	5.20
3	2.37	0.85	6.00
4	26.00	16.85	1.56
5	26.00	16.10	1.78

Table 14.5 Max displacement for *Y* direction unbalanced forces

Location	Displacement in *X* direction (mm)	Displacement in *Y* direction (mm)	Displacement in *Z* direction (mm)
1	0.21	2.00	0.25
2	0.12	0.12	0.23
3	0.12	0.14	0.50
4	2.03	1.25	1.38
5	2.13	1.30	1.30

Table 14.6 Max displacement for Z direction unbalanced forces

Location	Displacement in *X* direction (mm)	Displacement in *Y* direction (mm)	Displacement in *Z* direction (mm)
1	0.47	0.15	5.40
2	0.58	0.43	5.90
3	0.58	0.28	4.80
4	5.40	2.81	4.40
5	5.30	3.45	4.10

14.7.3 Max Displacement Plots for X Direction Unbalanced Forces

A max displacement of 26 mm was observed in the *X* direction at locations 4 and 5. In *Y* direction, max displacement observed was 17 mm at location 4. Max displacement of 6 mm observed in *Z* direction at location 3 (Figs. 14.6, 14.7 and 14.8).

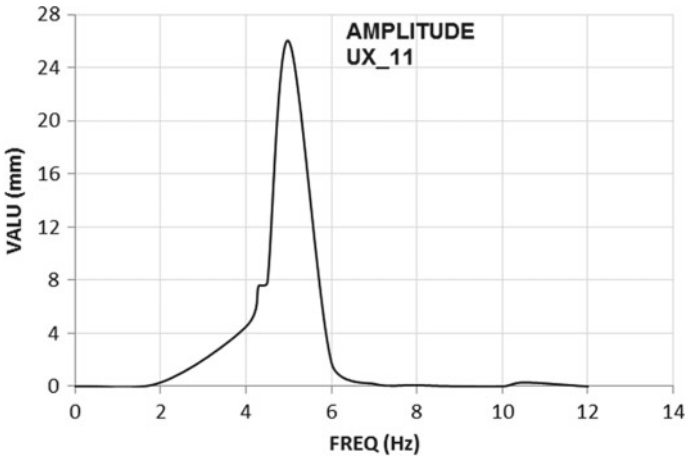

Fig. 14.6 Max *X* displacement versus frequency

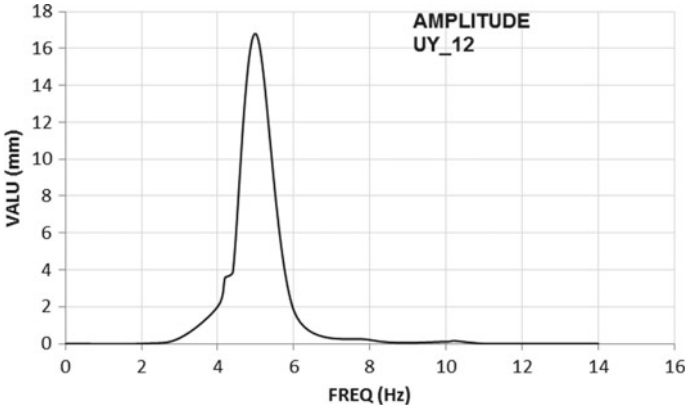

Fig. 14.7 Max versus displacement versus frequency

14.7.4 Max Displacement Plots for Y Direction Unbalanced Forces

A max displacement of 2.13 mm was observed in the *X* direction at location 5. In *Y* direction, max displacement observed was 2 mm at location 1. Max displacement of 1.38 mm observed in *Z* direction at location 4 (Figs. 14.9, 14.10 and 14.11)

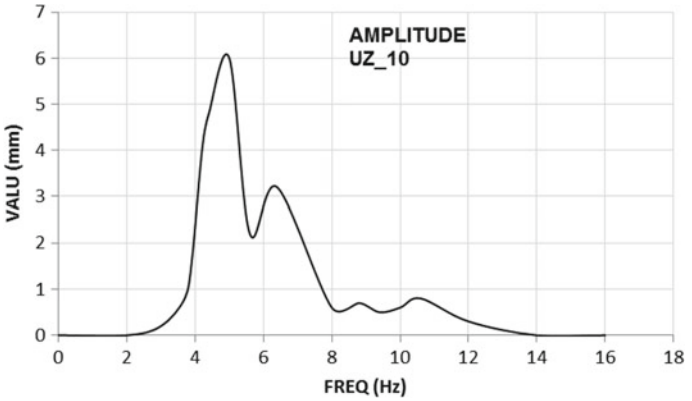

Fig. 14.8 Max *Z* displacement versus frequency

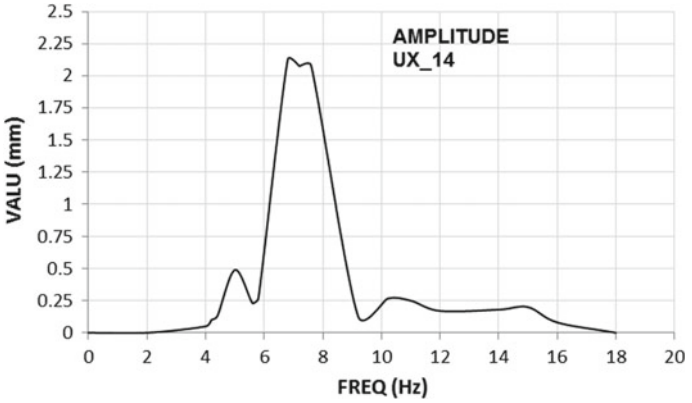

Fig. 14.9 Max *X* displacement versus frequency

14.7.5 Max Displacement Plots for Z Direction Unbalanced Forces

A max displacement of 5.4 mm was observed in the *X* direction at location 4. In *Y* direction, max displacement observed was 3.45 mm at location 5. Max displacement of 5.9 mm observed in *Z* direction at location 2 (Figs. 14.12, 14.13 and 14.14).

The locations 4 and 5 were experiencing high dynamic displacements. The maximum peak dynamic displacements in *X* direction was 26 mm. The maximum peak dynamic displacement in *Y* direction was 17 mm. The *X* and *Y* direction peak displacements were observed in the crusher maintenance enclosure.

The maximum *Z* direction displacement was observed in location 3. The location 3 belongs to feed hopper tip of crane side. The maximum *Z* direction displacement

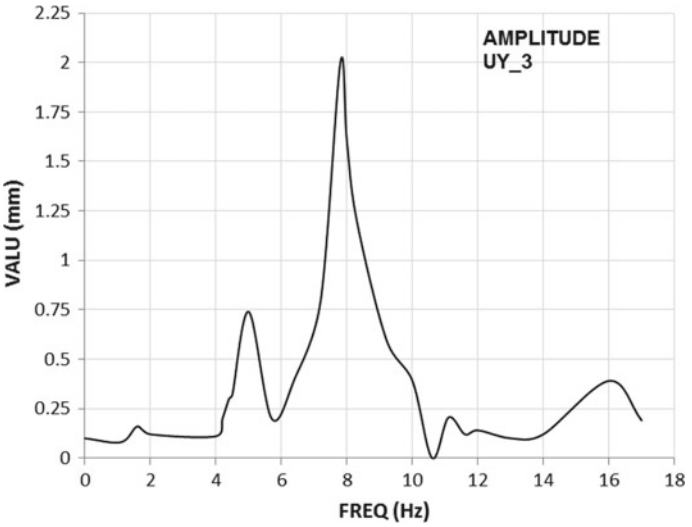

Fig. 14.10 Max *Y* displacement versus frequency

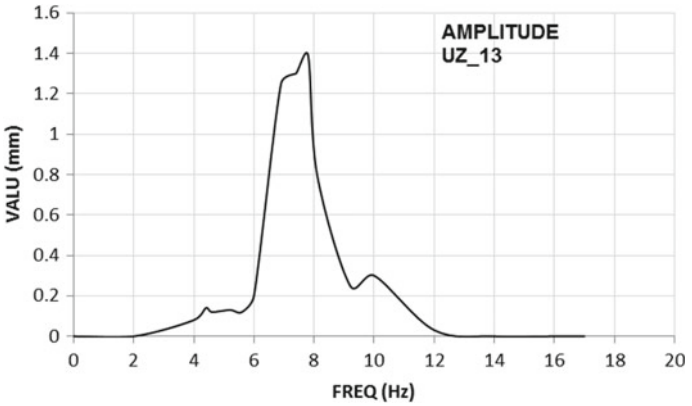

Fig. 14.11 Max *Z* displacement versus frequency

was 6 mm. Also, the analysis performed by applying the crusher unbalanced loads in the *Y* and *Z* direction.

The peak dynamic displacements in all three directions were found to be lesser than the unbalanced load applied in the *X* direction. The next weaker direction was *Z* as the displacements and stresses were very low in the case of the unbalanced load applied in the *Y* direction.

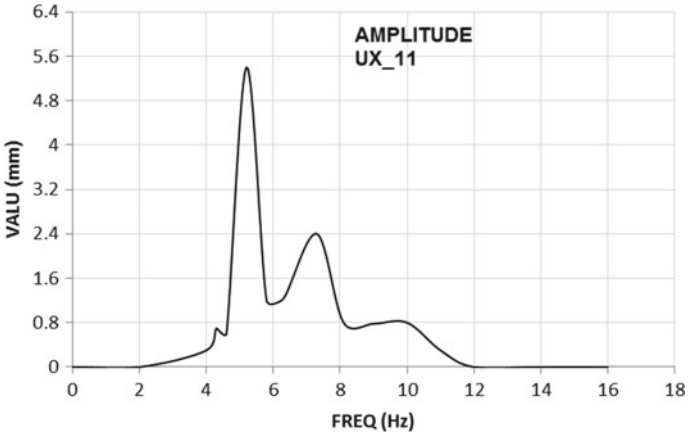

Fig. 14.12 Max *X* displacement versus frequency

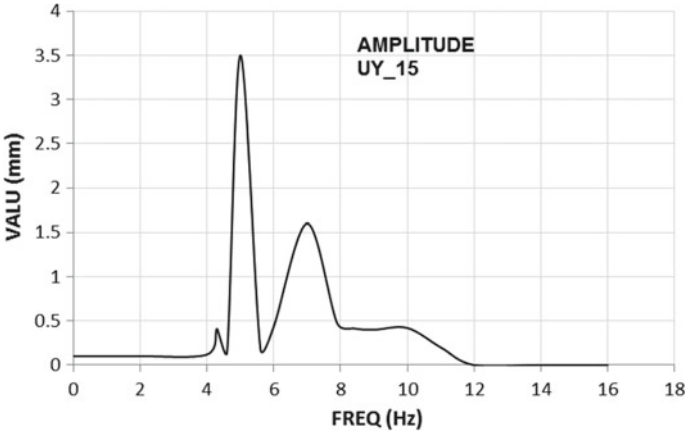

Fig. 14.13 Max *Y* displacement versus frequency

14.8 Conclusions

Having performed the analysis in all three directions, it was identified that the most critical/weak direction was *X* when compared to the other two. As expected, *Y* direction was very stiff when compared to the *Z* direction.

The *X* direction frequency response analysis results indicate that the most critical frequencies were 4.7, 4.8, 5.06 and 5.2 Hz. The analysis results indicate that resonance will not happen as the peak displacement was not observed near the excitation frequency of 2.34 Hz.

The critical frequencies observed in the crusher maintenance enclosure. Peak dynamic displacement in *X* direction was 26 mm observed in the crusher maintenance

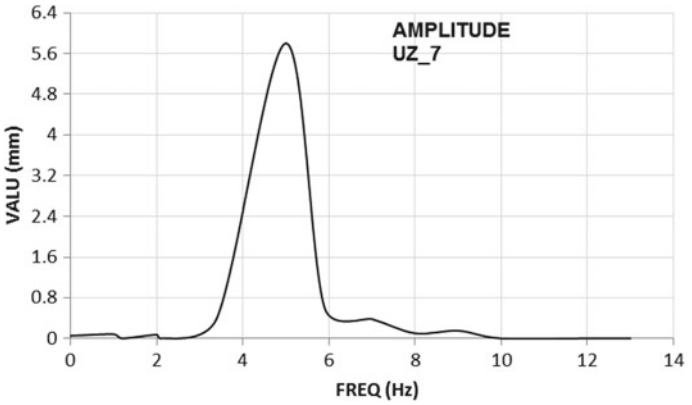

Fig. 14.14 Max *Z* displacement versus frequency

enclosure. Peak dynamic displacement in *Y* and *Z* direction was 17 and 6 mm, respectively, and considered to be acceptable based on L/D ratio and tests results conducted in the similar structure.

The peak dynamic displacement in *X* direction looks little high. It was suggested to lower the value below 20 mm by providing additional cross stiffeners and column bottom reinforcements. Allowable displacement criteria 20 mm was calculated based on the *L*/*D* ratio of the member location and tests results conducted in the similar structure. The hot spot stress observed in the bottom legs of the crusher maintenance enclosure. However, the stresses were lower than the endurance strength (150 MPa) of the material, and hence design was considered to be safe.

References

1. Modal analysis of Linear dynamic systems: Physical interpretation Anil K.Chopra, Member, ASCE
2. Dynamic analysis of structures. Athol J.Carr
3. Dynamic design and analysis method DDAM and Modal effective mass. Tone Abbey
4. He, J., Fu, Z.F.: Modal Analysis, 1st edn, p. 304. Butterworth-Heinemann, Oxford, Boston (2001). 10: 0080511783
5. Rao, S.S.: Mechanical Vibration, 4th edn. Pearson Education Press (2004)
6. Ansys® MAPDL Tutorials